Journal of
Stem Cell Research & Therapy

Jenner et al., J Stem Cell Res Ther 2014, 4:3
DOI: 10.4172/2157-7633.1000183

Research Article Open Access

Laser Capture Microdissection of Murine Interzone Cells: Layer Selection and Prediction of RNA Yield

Florien Jenner[1]*, Gerjo JVM van Osch[2], Mairead Cleary[2], Iris Ribitsch[1], Ulrich Sauer[3], René van Weeren[4] and Pieter Brama[5]

[1]*University of Veterinary Medicine Vienna, Equine Hospital, Vienna, Austria*
[2]*Erasmus MC, Department of Orthopaedics and Otorhinolaryngology, University Medical Center Rotterdam, Rotterdam, The Netherlands*
[3]*ZEISS Microscopy Labs, Munich, Germany*
[4]*Faculty of Veterinary Medicine, Department of Equine Sciences, Utrecht University, Utrecht, The Netherlands*
[5]*School of Veterinary Medicine, Section Veterinary Clinical Sciences, University College Dublin, Belfield, Dublin 4, Ireland*

Abstract

Objective: Articular chondrocytes originate from a distinct cohort of progenitor cells located in the so-called interzone in embryonic developing joints. We conducted this study 1) to determine if it is possible to identify the intermediate and outer interzone layers histologically (using cresyl violet) without adjunct in situ hybridization or immunohistochemistry; 2) to establish whether sufficient amounts of RNA can be harvested from each interzone layer of individual embryos to allow gene expression analysis; 3) to develop measurements that can provide an estimation of the RNA yield prior to costly amplification steps.

Methods: Cells from the outer (OI) and intermediate (II) interzone of the nascent femorotibial joint and the epiphyseal cartilage (EC) of femur and tibia of murine embryos of 13.5 and 15.5 days gestation were harvested using laser capture microdissection (LCM). Subsequently, microarray analysis was performed to confirm appropriate layer selection. The surface area harvested and the grey value (gv) of photomicrographs taken during LCM was measured and the corresponding relative optical density (ROD) was calculated and degree and significance of the correlation with RNA yield were determined.

Results: Cells from the OI, II and EC could be identified histologically using cresyl violet staining and were successfully harvested with LCM yielding sufficient amounts of RNA for linear amplification and microarray analysis. The RNA yield correlated significantly with the tissue surface area harvested, the mean gv and the corresponding ROD.

Conclusions: This study provides a technique for selective laser capture microdissection and subsequent microarray analysis of murine interzone cells of the intermediate and outer layer and presents a method to estimate the RNA yield by measuring the tissue area harvested and calculating the ROD. We recommend to harvest a minimum of 1×10^6 µm² of 13.5 days murine embryos and 3×10^6 µm² of 15.5 days murine embryos to obtain approximately 10 ng total RNA that can be used for linear T7-based amplification and subsequent microarray analysis.

Keywords: Joint development; Interzone; Cartilage; Chondrogenesis; Laser capture microdissection; Microarray; Optical density; RNA yield

Abbreviations: Anova: Analysis of Variance; Col2a1: Collagen II A1; EC: Transient Epiphyseal Cartilage; Gdf5: Growth/Differentiation Factor 5; gv: Grey Value; II: Intermediate Interzone; LCM: Laser Capture Microdissection; Matn1: Matrilin 1; OI: Outer Interzone; RIN: RNA Integrity Number; ROD: Relative Optical Density; Wnt9a: Wingless-type MMTV Integration Site Family Member 9A

Introduction

Articular chondrocytes originate from a distinct cohort of progenitor cells located in the interzone of developing embryonic joints [1]. This interzone is organized in three layers, 2 chondrogenic outer layers (outer interzone; OI) each facing the epiphyseal end of adjacent primordial long bones and a mesenchymal intermediate zone (intermediate interzone; II). Interzone cells can be distinguished from non-articular chondrocytes of the primordial limb by expression of markers such as growth/differentiation factor 5 (Gdf5), Wnt9a, and versican, whereas the expression of matrilin-1 (Matn1), a marker for transient epiphyseal chondrocytes, is absent in interzone cells [1-10].

Although the importance of the interzone for articular cartilage formation is well established, its exact role in the regulation of development and maintenance of the permanent articular chondrocytic phenotype remains unclear. To date the interzone's biological properties and possible functions have been largely inferred from research on embryos, rather than on isolated interzone cells themselves [1]. Targeted and separate harvesting of interzone cells provides an excellent tool to investigate cellular and molecular mechanisms of interzone cells that govern joint development and direct the formation of permanent or transient cartilage. To our knowledge only one report exists of interzone cell isolation [1]. In that study isolation of interzone cells was achieved by injection of a dye (Dil) and manual microdissection [1].

Laser Capture Microdissection (LCM) allows precise extraction of target cells from a heterogeneous tissue sample and can therefore

***Corresponding author:** Florien Jenner, University of Veterinary Medicine Vienna, Equine Hospital, Vienna, Austria, Tel: 431250775500; E-mail: florien.jenner@vetmeduni.ac.at

Received February 18, 2014; **Accepted** March 20, 2014; **Published** March 22, 2014

Citation: Jenner F, van Osch GJVM, Cleary M, Ribitsch I, Sauer U, et al. (2014) Laser Capture Microdissection of Murine Interzone Cells: Layer Selection and Prediction of RNA Yield. J Stem Cell Res Ther 4: 183. doi:10.4172/2157-7633.1000183

be considered a potentially interesting technique for the isolation of interzone cells [11]. However, correct identification of the cells of interest based on their morphologic characteristics is essential for successful isolation and a significant limiting factor for use of LCM in tissues such as the interzone so far [12]. Further, isolating specific cell types by LCM generally generates only low yields of RNA, potentially limiting its use for gene expression analysis of tissues. Consequently, LCM-coupled microarray studies typically require RNA amplification steps prior to microarray hybridization [11]. In this respect, a method to estimate whether the material collected contains sufficient RNA for linear amplification and downstream microarray analysis prior to undergoing costly amplification and labeling steps, would be very useful [11].

The first objective of the presented study was to investigate the accuracy of identification of the outer and intermediate interzone layer for subsequent harvesting of tissue samples by LCM based solely on histology with RNA-preserving staining techniques.

The second objective was to develop a method that utilizes the surface area harvested and the Relative Optical Density (ROD) of the tissue to predict RNA yield during the LCM isolation process.

Materials and Methods

Tissue preparation

Timed pregnant CD-1 IGS mice were purchased from Charles River laboratories (Sulzbach, Germany and Margate, UK). Embryos were recovered on gestational days 13.5 (E13.5) and 15.5 (E15.5), where noon of the day the vaginal plug was detected was designated as embryonic day 0.5. Limbs were staged according to Wanek et al. [13], dissected in ice-cold PBS, snap frozen in liquid nitrogen and stored at -80°C.

This study was approved by the institutional animal research ethics committee of University College Dublin (AREC-P-10-47).

Sample groups

The 6 sample groups were defined by tissue type and age. Epiphyseal cartilage (EC) and inner (II) and outer (OI) layer of the knee interzone were harvested from E13.5 and E15.5 mice. The gestational ages included in this study were chosen based on developmental criteria. At E13.5, the knee interzone is first morphologically detectable [3] and Matn-1 expression in the epiphyseal cartilage commences [1-3]. At E15.5, cavitation of the knee joint, and with it the next step in joint formation, begins [1-3]. To minimize variation due to differences in breeding and developmental timing, only limbs of 2 predetermined Wanek stages for each gestational age group (stage 7-8 for E13.5 and stage 11-12 for E15.5) were used for this experiment.

Laser capture microdissection (LCM)

Limbs were placed in the cryostat chamber for temperature equilibration, embedded in frozen section medium (Neg-50, ThermoFisher, Walldorf, Germany) and sectioned along their sagittal axis using a cryostat (Hyrax C 50 Cryostat, Carl Zeiss Microscopy GmbH, Jena, Germany) at a -25°C chamber/chuck temperature. Sections (10 µm) were mounted onto pre-cooled RNAse-free polyethylene naphthalate (PEN)-coated slides (Zeiss MembraneSlide 1.0 PEN NF, Carl Zeiss Microscopy GmbH) and stained with cresyl violet. On stained sections, the border between the light-stained interzone and dark-stained cartilage and bone condensations was readily distinguishable at 50x magnification (Figure 1). The layers of the interzone and epiphyseal cartilage were identified at 100x to 200x magnification. The outer layer of the interzone has a higher cell density and shows a curved configuration around the distal femur and proximal tibia (Figure 1). The cells of the interzone's intermediate layer are more loosely arranged and not clearly oriented toward either bone (Figure 1). The epiphyseal cartilage was sampled at a site equidistant from the outer interzone and the primary ossification center.

Laser capture microdissection was performed with the PALM MicroBeam system (Carl Zeiss Microscopy GmbH) equipped with an inverted microscope (Axio Observer, Carl Zeiss Microscopy GmbH), a CCD color camera (Axio Cam ICc1, Carl Zeiss Microscopy GmbH) and a motorized, computer controlled microscope stage and collection mechanism (CapMover, Carl Zeiss Microscopy GmbH). Each region of interest (EC, II, OI) was individually traced freehand on the touchpad screen (PL-2200, Wacom, Krefeld, Germany) in PALM Robosoftware (Carl Zeiss Microscopy GmbH), using different color tracing for each tissue type (Figure 1). Then, using the RoboLPC laser function, the ultraviolet laser beam cut along the predetermined path, dissected the regions of interest by color code and catapulted the selected tissues of each sample group directly into separate 500 µl Adhesive Cap tubes (Carl Zeiss Microscopy GmbH), avoiding contact and thereby RNase contamination. The harvested cells were lysed for 30 minutes using RLT lysis buffer (RNeasy® Micro kit, Qiagen Sciences Inc., Hilden, Germany), then vortexed and frozen at -20°C.

Three independent biological replicates were collected for each cell type (EC, II, OI). Each replicate originated from a different litter. The samples for E15.5 were obtained from individual embryos, for E13.5 samples we pooled two individuals per litter to get sufficient material for microarrays. Total RNA was extracted from cell lysates using RNeasy Micro Kits (Qiagen Sciences Inc.) according to manufacturer's protocols. RNA integrity, purity and quantity was determined and

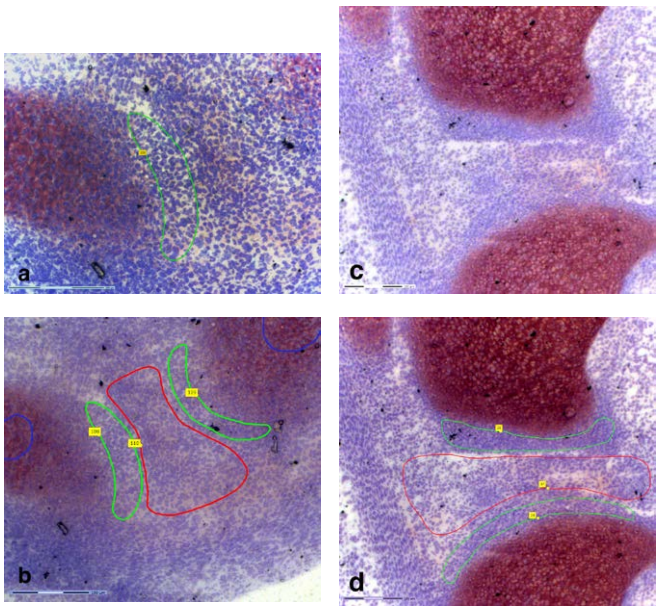

Figure 1: Micrographs of the (incipient) knee joint of a 13.5 day murine embryo (a and b) and a 15.5 day murine embryo (c and d) obtained during laser microdissection. The area outlined in red was considered to be the intermediate layer of the interzone; the area outlined in green was the outer layer of the interzone and blue indicated epiphyseal cartilage. The top left micrograph (a) was taken at 200x magnification, all others (b, c, d) were taken at 100x magnification (see scale bar in bottom left corner of each image).

expressed as RNA integrity number (RIN) with an Agilent Bioanalyzer 2100 (RNA 6000 Pico LabChip® Kit, Agilent Technologies, Waldbronn, Germany). RNA was stored at -80°C.

Microarrays

Each RNA sample was amplified and labeled using the Agilent Low Input Quick Amp Labeling Kit (Agilent Technologies) following the manufacturer's protocol, to produce Cyanine 3-CTP (Cy-3) labeled cRNA. Yields of cRNA and dye incorporation rate were measured with a NanoDrop ND-1000 UV-Vis Spectrophotometer (NanoDrop Technologies, Wilmington, USA).

Labeled cRNA was hybridized to Agilent Whole Mouse Genome Oligo Microarrays (Agilent SurePrint G3 Mouse 8x60L Microarray, Agilent Technologies). Hybridizations were performed by MiltenyiBiotec (BergischGladbach, Germany) according to the Agilent 60-mer microarray processing protocol. In brief, Cy-3 labeled fragmented cRNA in hybridization buffer was hybridized overnight (17 hours, 65°C) using the Agilent Gene Expression Hybridization Kit and Agilent's recommended hybridization chamber and oven. Following hybridization, the arrays were washed using the Gene Expression Wash Buffer 1 at room temperature and Buffer 2 at 37°C (Agilent #5188–5325, #5188–5326) for 1 min each. The last washing step was performed with acetonitrile. Fluorescence signals of the hybridized microarrays were detected using Agilent's Microarray Scanner System. The Agilent Feature Extraction Software was used to read out and process the microarray image files. The software determines feature intensities (including background subtraction), rejects outliers and calculates statistical confidences.

Determination of optical density of histological images and relation to RNA yield

Prior to laser microdissection, micrographs of cresyl violet stained sections with the regions of interest outlined, were taken under brightfield illumination. The RGB color images were converted to 8-bit greyscale (256 grey levels, 0= white, 255=black) and the mean grey value (gv) was measured for the entire image and the individual regions of interest using ImageJ software (version 1.45, National Institute of Health, USA). The relative optical density (ROD) was calculated using the formula ROD = $\log_{10}(255/255\text{-gv})$ [14].

The RNA concentration of each tissue sample, measured using the Agilent Bioanalyzer 2100 (RNA 6000 Pico LabChip® Kit, Agilent Technologies), was multiplied with the elution volume used for RNA extraction (12 µl) to calculate total RNA yield of each sample (Table 1). The total RNA yield was then divided by the surface area harvested to determine the tissue's RNA concentration. The minimum harvest surface area required to obtain 10 ng total RNA, the typical amount recommended for linear amplification, was also computed for each sample (Table 2). The correlation between embryo age, RNA yield, mean normalized signal intensity on the microarray, tissue RNA concentration, ROD and the product of area and gv as well as area and ROD was calculated using GraphPad Prism software (version 5.0d, GraphPad Software Inc., La Jolla, CA, USA). Two-way analysis of variance (ANOVA) assessed ROD and RNA concentration variables attributable to the tissue type and embryo age. Statistical significance was attributed to P values <0.05.

age group	tissue group	litter ID	embryo ID	tissue area harvested [µm²]	RIN	RNA harvested [ng]	cRNA [ng]	dye incorp. [fmol/ng]
13.5 days gestation	II	13.5-1	13.5-1-1	455829	9	4.34	950.94	12.49
			13.5-1-4	900000	8.9	4.91		
		13.5-2	13.5-2-1	216205	1.5	1.66	570.00	17.13
			13.5-2-4	479962	8.2	2.80		
		13.5-4	13.5-4-1	1738221	8.6	19.67	1952.10	14.80
			13.5-4-2	1021397	8.9	7.81		
	OI	13.5-1	13.5-1-1	317121	na	2.16	1131.03	13.37
			13.5-1-4	720000	8.2	6.10		
		13.5-2	13.5-2-1	236742	1.6	2.15	611.55	13.69
			13.5-2-4	306876	8.9	5.32		
		13.5-4	13.5-4-1	1032708	8.6	10.98	1593.00	12.54
			13.5-4-2	938646	9.1	11.42		
	EC	13.5-1	13.5-1-1	306100	7.4	3.44	1139.67	13.03
			13.5-1-4	840000	7.5	10.08		
		13.5-2	13.5-2-1	590909	4.2	4.88	731.70	12.55
			13.5-2-4	329599	7.9	8.88		
		13.5-4	13.5-4-1	712753	7.3	10.96	1296.27	13.33
			13.5-4-2	926888	8.4	15.04		
15.5 days gestation	II	15.5-1	15.5-1-1	917089	9.3	1.93	660.00	14.00
		15.5-2	15.5-2-6	1560000	9.5	5.87	1636.74	13.53
		15.5-3	15.5-3-2	2484543	6.1	7.48	3630.00	15.00
	OI	15.5-1	15.5-1-1	505786	6.2	1.64	490.00	13.00
		15.5-2	15.5-2-6	1430000	8.9	11.03	1551.96	13.57
		15.5-3	15.5-3-2	1354996	6.5	5.72	910.00	13.00
	EC	15.5-1	15.5-1-1	1662168	6.5	5.21	730.00	12.00
		15.5-2	15.5-2-6	3470000	7.8	6.79	1356.21	12.14
		15.5-3	15.5-3-2	4206940	6.7	23.51	1710.00	13.00

List of tissue area harvested and the amount of RNA extracted from each embryo and each tissue type (intermediate interzone (II), outer interzone (OI) and epiphyseal cartilage (EC)). The RIN value of the RNA, the resulting cRNA and the dye incorporation after T7 amplification are also indicated

Table 1: Tissue area harvested and amount of RNA extracted per embryo and tissue type.

	13.50				15.50			
	II	OI	EC	all zones	II	OI	EC	all zones
Mean	1.34	0.95	0.72	1.01	3.58	2.25	3.36	3.06
Std. Dev.	0.30	0.27	0.12	0.35	1.07	0.90	1.67	1.25
Min	1.00	0.73	0.63		2.66	1.30	1.79	
Max	1.56	1.26	0.85		4.75	3.08	5.11	

The calculated harvest surface area [mm²] required to obtain 10 ng total RNA from 10 µm thick sections depending on age (13.5 and 15.5 days of gestation) and tissue type (intermediate interzone (II), outer interzone (OI) and epiphyseal cartilage (EC)). While RNA yield is not significantly influenced by tissue type, 70.01% of RNA yield variation is attributable to embryonic age.

Table 2: Harvest surface area required to obtain 10 ng total RNA.

Results and Discussion

Accuracy of histological identification and isolation of interzone layers with LCM

The layers of the interzone and the transient epiphyseal cartilage were readily identifiable on cresyl violet stained sections based on their cell density, cell morphology and cellular arrangement, such as the outer interzone layer's distinct arrangement covering the opposing surfaces of the cartilaginous anlagen of femur and tibia (Figure 1). Gdf5, Versican, Wnt9a, Col2a1 and Matn1 signal intensity values of the different tissue layers selected and isolated by LCM are presented in Figure 2. The pattern of gene expression of known interzone marker genes Gdf5, Versican and Wnt9a and the low expression of Col2a1 and Matn1 compared to epiphyseal cartilage confirmed appropriate layer selection during LCM. As expected, the epiphyseal cartilage highly expressed Matn1 and Col2a1 and the interzone layers highly expressed Gdf5, Versican and Wnt9a. Surprisingly, both interzone layers of both age groups expressed some Matn1 and Col2a1, albeit at low levels. Based on published in situ hybridization (ISH) and lineage tracing studies Matn1 should only be expressed in the epiphyseal cartilage, but not in articular cartilage or its progenitors. We also unexpectedly found Col2a1 expressed in the intermediate layer of the interzone, which at E13.5 should already have reverted from its chondrogenic phenotype and ceased Col2a1 expression. Although contamination of the outer interzone samples with epiphyseal cartilage cannot be fully excluded as a consequence of its vicinity to the epiphyseal cartilage and the indistinct borders, contamination of the intermediate layer of the interzone with epiphyseal cartilage is highly unlikely. Because both layers of the interzone show some expression of Matn1, this strongly indicates Matn1 and Col2a1 are expressed in the interzone, albeit at very low levels. So far gene expression of the interzone has only been studied by ISH techniques and although these techniques are highly appropriate for gene expression profiling it is known that PCR and microarray techniques have a higher sensitivity [15-17]. In support of this another study looking at gene expression of articular cartilage compared to growth plate cartilage also found Matn1 expression in healthy articular cartilage of 2 week old mice [18]. The articular cartilage samples, harvested with LCM from the superficial two cell layers, expressed Matn1 at 10 fold lower level than growth plate cartilage levels, a similar proportion as the maximum we have found in the interzone compared to epiphyseal cartilage [18].

RNA yield and quality after LCM dissection

RNA quality of most embryonic samples was very good (RIN 6.5 – 9.5, Figure 3) and did not show any statistically significant correlation with RNA yield, tissue type or embryonic age (Table 1). Two E13.5 II samples had poor Bioanalyzer results – one showed no reading and the other had a measured RIN value of 1.6. Since both samples had very low RNA yields (2.16 and 2.15 ng respectively) and showed no signs of RNA degradation, the poor readings were attributed to insufficient RNA quantities for adequate measurements. The quantity and quality of RNA could have been decreased by staining as well as heat of the microscope lamp, both of which are unavoidable for identification of tissue morphology during laser microdissection [19]. Especially aqueous stains have been shown to cause significant RNA degradation [20]. Cresyl violet staining is an alcohol based staining technique and a well-established staining method for laser capture microdissection and subsequent microarray analysis [19]. To determine the tissue's inherent RNA concentration and quality as well as the effect of staining and microscope light exposure, RNA was extracted from unstained limb sections and from stained sections after 3 hours under the microscope in the course of a pilot study. The comparison of RNA obtained from unstained control sections and cresyl violet stained sections demonstrated no significant influence of staining on RNA quality (Figure 3). Three hours under the laser dissecting system's microscope resulted in only a small decrease in RNA quality and therefore this protocol seems well suited for LCM of embryonic interzones.

LCM and prediction of RNA yield

Although the interzone area in murine embryos is very small and yielded as little as 1.6 ng per sample, linear T7-based amplification

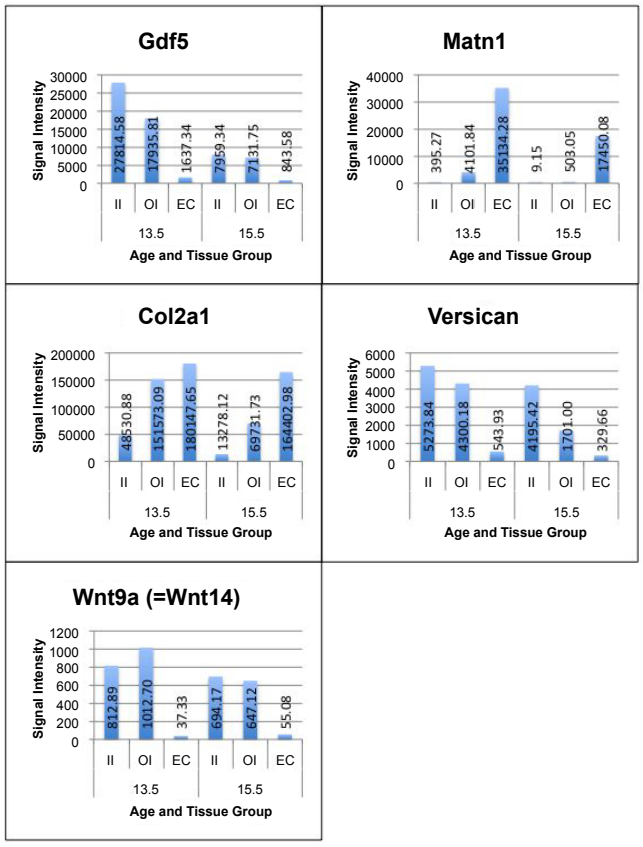

Figure 2: Chart comparing the gene expression of Col2a1, Gdf5, Matn1, Versican and Wnt 9a (=Wnt 14) in the various sample groups. Each bar represents the average signal intensity (y-axis) of the three biological replicates of each tissue and age group (x-axis). The relative signal intensities of the three tissue types of each individual mouse embryo (biological replicate) are well exemplified by this representation of the average.

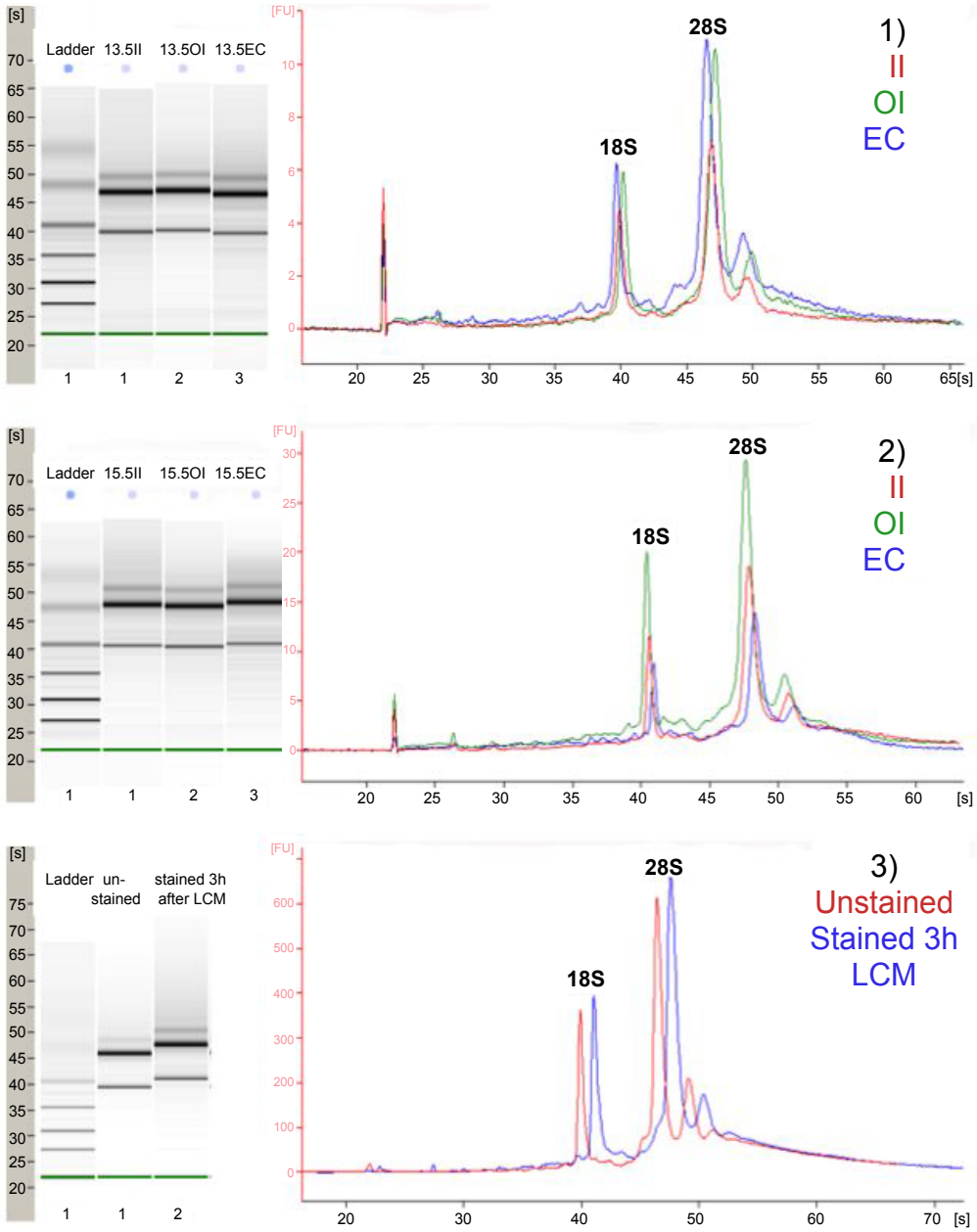

Figure 3: Representative Bioanalyzer electropherograms (fluorescence [ordinate] vs. time [abscissa]) with respective gels are shown for RNA extracted from
1) E13.5 intermediate ("II", RIN: 8.9, RNA concentration: 651 pg/µl, area harvested: appr. 1021000 µm²) and outer interzone ("OI", RIN: 9.1, RNA concentration: 952 pg/µl, area harvested: appr. 940000 µm²) and epiphyseal cartilage ("EC", RIN: 8.4, RNA concentration: 1253 pg/µl, area harvested: appr. 930000 µm²) (top)
2) E15.5 intermediate (RIN: 9.5, RNA concentration: 489 pg/µl, area harvested: appr. 1560000 µm²) and outer interzone (RIN: 8.9, RNA concentration: 919 pg/µl, area harvested: appr. 1430000 µm²) and epiphyseal cartilage (RIN: 7.8, RNA concentration: 566 pg/µl, area harvested: appr. 3470000 µm²) (middle)
3) A fresh unstained limb section (RIN: 10, RNA concentration: 30310 pg/µl) and stained limb section after 3 hours under the microscope (RIN: 9.4, RNA concentration: 40397 pg/µl) of an E14.5 (bottom).
Positions of 18S and 28S ribosomal RNA are indicated.

produced sufficient Cy3-labeled cRNA for subsequent microarray analysis. To develop a guide for the adequacy of the harvested samples, we established the correlation between measurable experimental variables, such as the surface area harvested and the gv of the LCM slides.

RNA yield showed a positive correlation with the surface area harvested (r=0.508, p=0.031). RNA yield also correlated with the $\log_{10}$cRNA (r=0.4943, p=0.037). Although neither correlation is particularly strong it can help to determine how much tissue must be collected to obtain sufficient RNA for linear amplification. Measuring the gv and calculating the ROD will further improve the estimate of RNA yield, as the correlation of total RNA yield per sample with the product of harvest surface area and gv (r=0.5232, p=0.0001) as well as with the product of harvest surface area and ROD (r=0.4609, p=0.0007) was stronger than with just area alone.

RNA concentration was not significantly influenced by tissue type but 70% of variance in RNA yield was attributable to embryonic age (two-way ANOVA: $p<0.0001$). Embryos of age E13.5 yielded more RNA per tissue surface area than of age E15.5. There was also a statistically significant association between ROD, zone and embryonic age (two-way ANOVA: $p<0.0001$), with zone accounting for 42% and embryo age for 49% of variation in ROD. Although embryo age accounts for a significant proportion of the total variance in RNA yield and ROD, neither RNA yield nor ROD showed a significant correlation with embryo age.

Since an average microarray experiment requires 10–100 µg of labeled cRNA, an amount far out of reach of most cell and tissue specific studies, linear amplification is often unavoidable in laser microdissection based microarray studies [21]. Linear T7-based amplification and its implications for data analysis have therefore been extensively studied and proven not to have any systematic influence on the outcome of the microarray experiment or affect the selection of differentially expressed genes, provided all samples included in the study are equally treated and amplified [21,22]. Typically, total RNA amounts of a minimum of 10ng are recommended as starting material for T7-based linear amplification [23]. As LCM is time consuming and downstream linear amplification and microarray analysis are costly, correct assessment of the adequacy of the harvested tissue's RNA yield is important. Measuring the gv of the slide's area of interest as well as the surface area harvested and calculating the ROD can help with that assessment during the harvesting procedure, thus granting the opportunity to continue cell harvest if the yield appears to be insufficient and vice versa stop the LCM when adequate amounts have been obtained. The required harvest surface area to obtain adequate amounts of RNA is dependent on the cellular density of each tissue type and hence is tissue specific. The calculated harvest surface area required to obtain 10 ng total RNA is detailed by age and zone in Table 2. Based on our results we recommend to harvest a minimum of 1×10^6 µm^2 of E13.5 and 3×10^6 µm^2 of E 15.5 interzone or epiphyseal cartilage.

Conclusions

This study provides a technique for selective LCM and subsequent microarray analysis of cells from the intermediate and outer layers of the murine interzone. It also provides a method to estimate the RNA yield before dissection by measuring the tissue area selected for harvesting and the grey value of the LCM slide and calculating the ROD.

We would recommend to harvest a minimum of 1×10^6 µm^2 of E13.5 and 3×10^6 µm^2 of E 15.5 to obtain approx. 10 ng total RNA, which is sufficient for linear T7-based amplification and subsequent microarray analysis.

Acknowledgments

Many thanks toLukas Baran of Zeiss Microscopy Labs Munich for his assistance with laser microdissection and to John Breteler for his help with sample harvesting.

References

1. Koyama E, Shibukawa Y, Nagayama M, Sugito H, Young B, et al. (2008) A distinct cohort of progenitor cells participates in synovial joint and articular cartilage formation during mouse limb skeletogenesis. DevBiol 316(1): 62-73. [Pubmed]
2. Hyde G, Boot-Handford RP, Wallis GA (2008) Col2a1 lineage tracing reveals that the meniscus of the knee joint has a complex cellular origin.J Anat213(5): 531–538. [Pubmed]
3. Hyde G, Dover S, Aszodi A, Wallis GA, Boot-Handford RP (2007)Lineage tracing using matrilin-1 gene expression reveals that articular chondrocytes exist as the joint interzone forms. Dev Biol 304(2): 825–833.[Pubmed]
4. Rountree RB, Schoor M, Chen H, Marks ME, Harley V, et al. (2004) BMP receptor signaling is required for postnatal maintenance of articular cartilage. Plos Biol 2: e355.[Pubmed]
5. Francis-West PH, Parish J, Lee K, Archer CW (1999) BMP/GDF-signalling interactions during synovial joint development. Cell Tissue Res 296(1): 111–119.[Pubmed]
6. Storm EE, Kingsley DM (1996) Joint patterning defects caused by single and double mutations in members of the bone morphogenetic protein (BMP) family. Development 122(12): 3969–3979.[Pubmed]
7. Storm EE, Kingsley DM (1999) GDF5 coordinates bone and joint formation during digit development. Dev Biol 209(1): 11–27.[Pubmed]
8. Snow HE, Riccio LM, Mjaatvedt CH, Hoffman S, Capehart AA (2005) Versican expression during skeletal/joint morphogenesis and patterning of muscle and nerve in the embryonic mouse limb. Anat Rec A Discov Mol Cell Evol Biol 282(2): 95–105.[Pubmed]
9. Shepard JB, Krug HA, LaFoon BA, Hoffman S, Capehart AA (2007) Versican expression during synovial joint morphogenesis. Int J Biol Sci 3(6): 380–384. [Pubmed]
10. Pitsillides AA, Beier F (2011) Cartilage biology in osteoarthritis—lessons from developmental biology. Nat Rev Rheumatol 7(11): 654–663.[Pubmed]
11. Klee EW, Erdogan S, Tillmans L, Kosari F, Sun Z, et al. (2009) Impact of sample acquisition and linear amplification on gene expression profiling of lung adenocarcinoma: laser capture micro-dissection cell-sampling versus bulk tissue-sampling. BMC Med Genomics 2: 13–13.[Pubmed]
12. Espina V, Wulfkuhle JD, Calvert VS, VanMeter A, Zhou W, et al. (2006) Laser-capture microdissection. Nat Protoc 1(2): 586–603.[Pubmed]
13. Wanek N, Muneoka K, Holler-Dinsmore G, Burton R, Bryant SV (1989) A staging system for mouse limb development. J Exp Zool 249(1): 41–49. [Pubmed]
14. Vizi S, Palfi A, Hatvani L, Gulya K (2001) Methods for quantification of in situ hybridization signals obtained by film autoradiography and phosphorimaging applied for estimation of regional levels of calmodulin mRNA classes in the rat brain. Brain Res Brain Res Protoc 8(1): 32–44.[Pubmed]
15. Greene JG, Borges K, Dingledine R (2009) Quantitative transcriptional neuroanatomy of the rat hippocampus: Evidence for wide-ranging, pathway-specific heterogeneity among three principal cell layers. Hippocampus 19(3): 253–264.[Pubmed]
16. Lee C-K, Sunkin SM, Kuan C, Thompson CL, Pathak S, et al. (2008) Quantitative methods for genome-scale analysis of in situ hybridization and correlation with microarray data. Genome Biol 9(1): R23.[Pubmed]
17. Konig R, Baldessari D, Pollet N, Niehrs C, Eils R (2004) Reliability of gene expression ratios for cDNA microarrays in multiconditional experiments with a reference design. Nucleic Acids Res 32(3): 29e–29.[Pubmed]
18. Yamane S, Cheng E, You Z, Reddi AH (2007) Gene expression profiling of mouse articular and growth plate cartilage. Tissue Eng 13(9): 2163–2173. [Pubmed]
19. Aaltonen KE, Ebbesson A, Wigerup C, Hedenfalk I (2011) Laser capture microdissection (LCM) and whole genome amplification (WGA) of DNA from normal breast tissue --- optimization for genome wide array analyses. BMC Res Notes 4: 69.[Pubmed]
20. Kube D, Savci-Heijink C, Lamblin AF, Kosari F, Vasmatzis G, et al. (2007) Optimization of laser capture microdissection and RNA amplification for gene expression profiling of prostate cancer. BMC Mol Biol 8: 25.[Pubmed]
21. Schneider J, Buness A, Huber W, Volz J, Kioschis P, et al. (2004) Systematic analysis of T7 RNA polymerase based *in vitro* linear RNA amplification for use in microarray experiments. BMC Genomics 5(1): 29.[Pubmed]
22. Stemmer K, Ellinger-Ziegelbauer H, Lotz K, Ahr H-J, Dietrich DR (2006) Establishment of a protocol for the gene expression analysis of laser microdissected rat kidney samples with affymetrix genechips. Toxicol Appl Pharmacol 217(1): 134–142.[Pubmed]
23. Sengupta S, Ruotti V, Bolin J, Elwell A, Hernandez A, et al. (2010) Highly consistent, fully representative mRNA-Seq libraries from ten nanograms of total RNA. Biotech 49(6): 898–904.[Pubmed]